

## Distinctive Higgs Signals of a Type II 2HDM at the LHC

Shinya Kanemura<sup>1 \*</sup>, Stefano Moretti<sup>2 †</sup>, Yuki Mukai<sup>1 ‡</sup>, Rui Santos<sup>2 §</sup> and Kei Yagyu<sup>1 ¶</sup>

<sup>1</sup> *Department of Physics, University of Toyama, 3190 Gofuku, Toyama 930-8555, Japan.*

<sup>2</sup> *School of Physics and Astronomy, University of Southampton, Highfield, Southampton SO17 1BJ, UK.*

(Dated: April 22, 2019)

We perform a numerical analysis of Higgs-to-Higgs decays within a Type II 2-Higgs Doublet Model (2HDM), highlighting several channels that cannot occur in its Supersymmetric version, thereby allowing one to possibly distinguish between these two scenarios. Our results are compliant with all available experimental bounds from both direct and indirect Higgs searches and with theoretical constraints from vacuum stability and perturbative unitarity.

### I. INTRODUCTION

Whilst Supersymmetry (SUSY) [1] provides an attractive theoretical scenario for physics beyond the Standard Model (SM) (in its ability to remedy the hierarchy problem, to provide a natural dark matter candidate, to enable high scale gauge coupling unification, etc.), there is to date no evidence for it. In its minimal (in terms of particle content and gauge structure) incarnation, the Minimal Supersymmetric Standard Model (MSSM) [2], SUSY is highly predictive though, e.g., in the Higgs sector. Of the initial eight degrees of freedom pertaining to the two complex Higgs doublets responsible for Electro-Weak Symmetry Breaking (EWSB) in the MSSM, after the latter has taken place, three are consumed to give mass to the  $SU(2) \otimes U(1)$  weak gauge bosons,  $W^\pm$  and  $Z$ , so that five physical Higgs states survive: the CP-neutral ones  $h$  and  $H$  ( $M_H > M_h$ ), the CP-odd one  $A$  and the charged states  $H^\pm$ . In effect, limitedly to the Higgs sector, the MSSM is nothing but a 2-Higgs Doublet Model (2HDM) of Type II (in the nomenclature of Ref. [3]), whereby SUSY enforces relations amongst Higgs masses and couplings, on the one hand, and weak gauge boson masses and interaction parameters, on the other hand, in such a way that, of the original 7 independent parameters defining a CP-conserving 2HDM (see below), only two survive as such in the MSSM [4]. These can be taken to be  $\tan\beta$ , the ratio of the Vacuum Expectation Values (VEVs) of the two Higgs doublet fields, and one of the extra Higgs boson masses. At tree-level, these are the only inputs needed to compute Higgs masses and couplings to ordinary matter (quarks, leptons and gauge bosons) as well as Higgs self-couplings. Hence, if SUSY had chosen all the sparticle masses to be much larger than the SM objects and the Higgs bosons, so that they are not accessible at the upcoming Large Hadron Collider (LHC), one intriguing question to ask would be whether it is possible to distinguish between the MSSM and a Type II 2HDM on the sole basis of Higgs interactions with SM matter and/or self-interactions. Or, conversely, whether it would be possible to dismiss the assumption of such (decoupled) heavy sparticles, hence of minimal SUSY altogether (aka the MSSM), from the observation of particular signals in the Higgs sector alone.

It is the purpose of this letter to prove that this is the case, exploiting the fact that – in the light of all available experimental constraints – SUSY prevents some Higgs-to-Higgs decays, that remain instead possible in a generic Type II 2HDM. This is primarily connected to the fact that a generic pattern of Higgs masses, as dictated by SUSY, in the MSSM is the one in which the  $h$  is rather light (in fact, below  $130 \text{ GeV}$  or so, for heavy sparticles [5]) whilst the others ( $H$ ,  $A$  and  $H^\pm$ ) are quite heavy and degenerate in mass, the more so the larger  $\tan\beta$  [32]. In fact, even in the presence of off-shellness effects [6, 7] in all decay products in Higgs decay chains in the MSSM, essentially only the  $H \rightarrow hh$  and  $A \rightarrow Zh$  channels are possible in this scenario [33]. In contrast, in a Type II 2HDM without SUSY, for parameter

---

\* kanemu@sci.u-toyama.ac.jp

† stefano@phys.soton.ac.uk

‡ mukai@jodo.sci.u-toyama.ac.jp

§ rsantos@cii.fc.ul.pt

¶ keiyagyu@jodo.sci.u-toyama.ac.jp

configurations compliant with all available experimental bounds, one can also have, e.g.:

$$\begin{aligned}
H &\rightarrow AA, & H &\rightarrow H^+H^-, & H &\rightarrow W^\pm H^\mp, & H &\rightarrow ZA, \\
&& A &\rightarrow W^\pm H^\mp, & A &\rightarrow ZH, \\
H^\pm &\rightarrow W^\pm h, & H^\pm &\rightarrow W^\pm H.
\end{aligned} \tag{1}$$

While, of course, they could not occur all at the same time, depending on the Type II 2HDM parameters, a subset of these would be possible, therefore providing a means of distinguishing between the two scenarios discussed, further considering that – under the above assumption of a heavy SUSY spectrum – the dominant production channels of both neutral and charged Higgs bosons in both scenarios are the same and proceed via interactions with SM particles [8, 9].

The plan of the paper is as follows. In the next section we describe the Type II 2HDM that we will be using and we fix our conventions. The following section illustrates our results quantitatively. The final section outlines the conclusions.

## II. THE TWO-HIGGS DOUBLET MODEL

We start with a brief review of the 2HDM used in this work. The potential chosen is the most general, renormalisable and invariant under  $SU(2) \otimes U(1)$  that one can build with two complex Higgs doublets with a softly broken  $Z_2$  symmetry. It can be written as

$$\begin{aligned}
V_{\text{2HDM}} &= \mu_1^2 |\Phi_1|^2 + \mu_2^2 |\Phi_2|^2 - (\mu_3^2 \Phi_1^\dagger \Phi_2 + \text{h.c.}) \\
&\quad + \frac{1}{2} \lambda_1 |\Phi_1|^4 + \frac{1}{2} \lambda_2 |\Phi_2|^4 + \lambda_3 |\Phi_1|^2 |\Phi_2|^2 + \lambda_4 |\Phi_1^\dagger \Phi_2|^2 + \frac{\lambda_5}{2} \{ (\Phi_1^\dagger \Phi_2)^2 + \text{h.c.} \},
\end{aligned} \tag{2}$$

where  $\Phi_1$  and  $\Phi_2$  are the two Higgs doublets with hypercharge  $+1/2$  and  $\mu_3^2$  is the  $Z_2$  soft breaking term. For simplicity we can take  $\mu_3^2$  and  $\lambda_5$  to be real. The doublet fields are parameterised as

$$\Phi_i = \begin{bmatrix} \omega_i^+ \\ \frac{1}{\sqrt{2}}(v_i + h_i + iz_i) \end{bmatrix} \quad (i = 1, 2), \tag{3}$$

where the VEVs  $v_1$  and  $v_2$  satisfy  $v_1^2 + v_2^2 = v^2 \simeq (246 \text{ GeV})^2$ . Assuming CP-conservation, this potential has 8 independent parameters. However, because  $v$  is fixed by the  $W^\pm$  boson mass, only 7 independent parameters remain to be chosen, which we take to be  $M_h, M_H, M_A, M_{H^\pm}, \tan \beta, \alpha$  (the mixing angle between the two CP-even neutral Higgs states) and  $M^2 = \mu_3^2 / (\sin \beta \cos \beta)$  (which is a measure of how the discrete symmetry is broken). The definition of  $\alpha$  and  $\beta$  and the relation among physical scalar masses and coupling constants are shown in Ref. [10] for definiteness.

In a general 2HDM, the Yukawa Lagrangian can be built in four different and independent ways so that it is free from Flavour Changing Neutral Currents (FCNCs). We define as Type I the model where only the doublet  $\phi_2$  couples to all fermions; in a Type II model  $\phi_2$  couples to up-type quarks and  $\phi_1$  couples to down-type quarks and leptons; in a Type III [3] (also known as Type Y) model  $\phi_2$  couples to all quarks and  $\phi_1$  couples to all leptons; a Type IV [3] (also known as Type X [11]) model is instead built such that  $\phi_2$  couples to up-type quarks and to leptons and  $\phi_1$  couples to down-type quarks. (For completeness, we present the Yukawa couplings for a Type II 2HDM in the Appendix.)

## III. EXPERIMENTAL AND THEORETICAL BOUNDS

The results from all LEP collaborations on topological searches with two Higgs bosons or one Higgs and one gauge boson were presented in Ref. [12]. We will use the experimental limits on the cross sections for  $e^+e^- \rightarrow H_1 Z$  and  $e^+e^- \rightarrow H_1 H_2$ , where  $H_1$  can be any CP-even Higgs boson and  $H_2$  can be either a CP-even or a CP-odd Higgs boson. As we are concerned here with a Type II 2HDM, there is a bound particularly relevant to our analysis which is the one obtained from the relation involving the following cross sections ( $\sigma$ ) and Branching Ratios (BRs):

$$\frac{\sigma(e^+e^- \rightarrow H_1^{2\text{HDM}} Z)}{\sigma(e^+e^- \rightarrow H_1^{\text{SM}} Z)} \text{BR}(H_1^{2\text{HDM}} \rightarrow b\bar{b}) = \sin^2(\alpha - \beta) \text{BR}(H_1^{2\text{HDM}} \rightarrow b\bar{b}). \tag{4}$$

In a Type II 2HDM  $h \rightarrow b\bar{b}$  is the dominant decay for most of the parameter space for  $M_h$  below the SM limit. The two subleading competing decays are  $h \rightarrow c\bar{c}$  and  $h \rightarrow \tau^+\tau^-$ . In a Type II 2HDM, the ratio  $\Gamma(h \rightarrow b\bar{b})/\Gamma(h \rightarrow \tau^+\tau^-)$  is the SM one. In contrast, one has

$$\frac{\Gamma(h \rightarrow b\bar{b})}{\Gamma(h \rightarrow c\bar{c})} = \frac{m_b^2}{m_c^2} \tan^2 \alpha \tan^2 \beta \quad (5)$$

in the limit  $m_h \gg m_q$ . If we then take the case  $\alpha \approx \beta$  and because we always consider  $\tan \beta > 1$  the decay  $h \rightarrow b\bar{b}$  becomes even more dominant in a Type II 2HDM, with respect to the SM case. Conversely, if  $\alpha \approx \beta + \pi/2$ , then we recover the SM ratio. Either way,  $h \rightarrow b\bar{b}$  is the dominant decay by an amount which is least the corresponding SM ratio of BRs with respect to the other fermionic decays. Because its dependence on the other parameters of the model is very mild, this essentially provides a limit in the  $\beta - \alpha$  versus  $M_h$  plane. In particular, it is straightforward to check that when  $\sin(\beta - \alpha) \approx 0.1$  there is essentially no bound on the lightest Higgs boson mass, while for  $\sin(\beta - \alpha) \approx 0.2$  the limit immediately jumps to  $M_h > 75.6$  GeV.

In this study the masses of the charged Higgs boson and the CP-odd one will always be above 200 GeV and therefore not constrained at all by the LEP bounds from direct searches. In some cases though, the mass of the heavy CP-even Higgs boson will be allowed to be below 200 GeV. In those instances we have confirmed that the LEP bounds do not apply to the cases presented in this work. Concerning  $H^\pm$  states, apart from a model independent LEP bound of  $M_{H^\pm} \gtrsim M_{W^\pm}$ , D0 and CDF have model dependent limits on the charged Higgs mass (see Refs. [13]) from top decays, but again these are below the range of  $H^\pm$  masses discussed in this work. No other experimental bounds exist from direct searches for the set of parameters that we will present.

Other than limits from direct searches for Higgs bosons, there are indirect constraints from precision observables, from both LEP and SLC. New contributions to the  $\rho$  parameter stemming from Higgs states [14] have to comply with the current limits from precision measurements [15]:  $|\delta\rho| \lesssim 10^{-3}$ . There are limiting cases though, related to an underlying custodial symmetry, where the extra contributions to  $\delta\rho$  vanish. In this study we will consider two such particular cases: (A) the one where  $M_{H^\pm} = M_A$  and (B) the one where  $M_{H^\pm} = M_H$  with  $\sin(\beta - \alpha) = 1$ . These parameter choices correspond to the case in which the custodial symmetry ( $SU(2)_L \otimes SU(2)_R \rightarrow SU(2)_V$ ) is preserved in the Higgs potential, so that the Higgs potential can be written in terms of  $\text{Tr}(M_i M_i^\dagger)$  with  $M_i = (i\tau_2 \Phi_i^*, \Phi_i)$  where the  $M_i$ 's ( $i = 1, 2$ ) are translated as  $M_i \rightarrow M'_i = g_L^\dagger M_i g_R$  with  $g_{L,R} \in SU(2)_{L,R}$  (A) or  $\text{Tr}(M_{21} M_{21}^\dagger)$  and  $\det(M_{21})$ , with  $M_{21} = (i\tau_2 \Phi_2^*, \Phi_1)$ , where  $M_{21}$  is translated as  $M_{21} \rightarrow M'_{21} = g_L^\dagger M_{21} g_R$  with  $g_{L,R} \in SU(2)_{L,R}$  (B), respectively [16]. In Fig. 1, we show the allowed region under the  $\rho$  parameter constraint in several scenarios which are relevant to our later discussions. Furthermore, it has recently been shown in Ref. [17] that, for a Type II 2HDM, data on  $B \rightarrow X_s \gamma$  imposes a lower limit of  $M_{H^\pm} \gtrsim 250$  GeV, which is essentially  $\tan \beta$  independent. Other experimental constraints on a Type II 2HDM come from the results on  $(g-2)_\mu$  (the muon anomalous magnetic moment) [18],  $R_b$  (the  $b$ -jet fraction in  $e^+e^- \rightarrow Z \rightarrow \text{jets}$ ) [19, 20], the decay  $B^+ \rightarrow \tau^+\nu$  [21] and the  $\tau$  leptonic decay [22]. In general, bounds from these observables can be important for relatively small values of  $M_{H^\pm}$  and large  $\tan \beta \gtrsim 10$  [18, 19, 20, 21, 22, 23, 24]. In the following, we will consider  $M_{H^\pm}$  to be 250 GeV or larger and take  $\tan \beta \sim 1-3$ , so that all the Type II 2HDM scenarios in this Letter are free from these bounds.

Concerning theoretical constraints we will take all masses  $M_h$ ,  $M_H$ ,  $M_A$  and  $M_{H^\pm}$ , to be below 700 GeV. This is a consequence of tree-level unitarity bounds [25, 26] in the limit  $M = 0$ . Furthermore, the most general set of conditions for the Higgs potential to be bounded from below are [27]

$$\lambda_1 > 0, \quad \lambda_2 > 0, \quad \sqrt{\lambda_1 \lambda_2} + \lambda_3 + \min(0, \lambda_4 - |\lambda_5|) > 0. \quad (6)$$

Recently, it was in fact proven that these are necessary and sufficient conditions to assure vacuum stability of the potential at tree level [28]. Vacuum stability against charge breaking is also built into a Type II 2HDM model, as a non-charge breaking minimum, when it exists, is always the global one in any 2HDM [29]. Finally, according to [30], perturbativity for the top and bottom Yukawa couplings forces  $\tan \beta$  to lie in the range  $0.3 \leq \tan \beta \leq 100$ , though it turns out that, from enforcing perturbativity also on the  $\lambda_i$ 's, moderate values of  $\tan \beta$  ( $\tan \beta \sim \mathcal{O}(1)$ ) are preferred, especially for  $M \sim 0$  GeV.

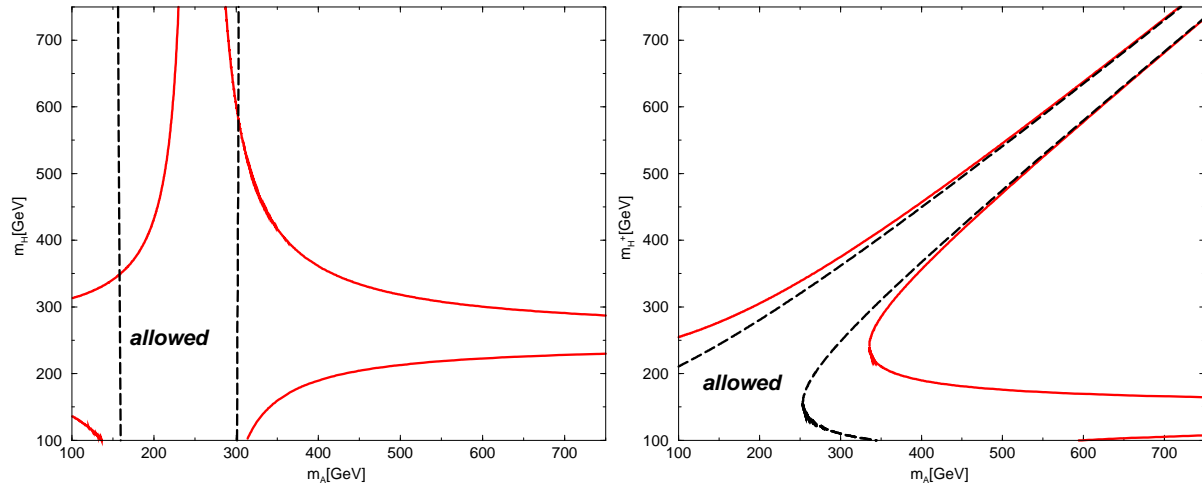


FIG. 1: Allowed regions under the  $\rho$  parameter data (at  $2\sigma$  level). [Left figure] The area surrounded by solid curves corresponds to the allowed regions for the case of  $M_h = 120$  GeV,  $M_{H^\pm} = 250$  GeV,  $\sin(\beta - \alpha) = 1$ . The one surrounded by dashed curves corresponds to the allowed regions for the case of  $M_h = 50$  GeV,  $M_{H^\pm} = 250$  GeV,  $\sin(\beta - \alpha) = 0.1$ . [Right figure] The area surrounded by solid curves corresponds to the allowed regions for the case of  $M_h = 120$  GeV,  $M_H = 150$  GeV,  $\sin(\beta - \alpha) = 0.9$ . The one surrounded by dashed curves corresponds to the allowed regions for the case of  $M_h = 50$  GeV,  $M_H = 150$  GeV,  $\sin(\beta - \alpha) = 0.1$ .

## IV. DECAYS

### A. $A$ decays

In the mass region chosen,  $\sin(\beta - \alpha)$  has to be very close to 1, in order for the model to be consistent with experimental data. Even a value of  $\sin(\beta - \alpha) = 0.9$  is enough to violate precision measurements via the  $\rho$  parameter. Therefore the decay  $A \rightarrow Zh$  is not allowed, despite we take  $M_h = 120$  GeV, and the CP-odd Higgs boson profile does not depend on the light CP-even Higgs boson mass. We have chosen  $M_H = M_{H^\pm} = 250$  GeV due to the  $B \rightarrow X_s \gamma$  bound and to the  $\rho$  constraint. Fig. 2 illustrates the decay patterns of the CP-odd Higgs state for two values of  $\tan\beta$ . Two comments are in order here. Firstly, notice that to choose larger values for  $M_H$  and  $M_{H^\pm}$  would only have the effect that the corresponding channels would open later. Secondly, the dependence on  $\tan\beta$  is generally as follows: the larger  $\tan\beta$  the

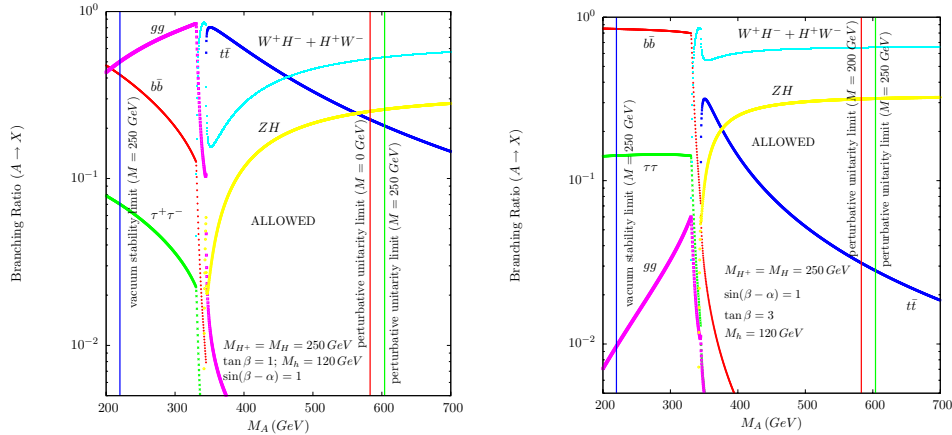


FIG. 2:  $A$  decays for  $M_h = 120$  GeV,  $M_H = M_{H^\pm} = 250$  GeV and  $\sin(\beta - \alpha) = 1$ . On the left is the plot for  $\tan\beta = 1$  while on the right we set  $\tan\beta = 3$ . We also show the perturbative unitarity and the vacuum stability limits, for  $M = 0$  GeV and  $M = 250$  GeV on the left plot and  $M = 0$  GeV,  $M = 200$  GeV and  $M = 250$  GeV on the right plot. For  $M = 0$  GeV and  $\tan\beta = 3$  there is no allowed region (right plot).

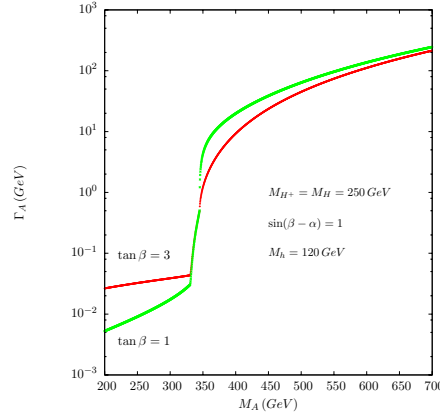


FIG. 3: Total width of the CP-odd Higgs state  $A$  for the parameter values presented in Fig. 2.

more suppressed the decay into  $t\bar{t}$  and consequently the CP-odd Higgs state decays more and more into other Higgs bosons as soon as the corresponding channels are kinematically allowed. All decay channels shown in these plots do not depend on  $M$ , as no Higgs self-couplings are involved in those processes. However, both the perturbative unitarity and the vacuum stability bounds depend on the value chosen for  $M$ . The dependence for the three values of  $M = 0, 200$  and  $250$  GeV is shown in Fig. 2. In Fig. 3 we show the total  $A$  width for the two situations presented in Fig. 2. When the  $A$  decays mainly to  $b\bar{b}$  or  $g\bar{g}$  the width is negligible but, when the  $t\bar{t}$ , the other Higgs or Higgs plus gauge boson channels open,  $\Gamma_A$  grows rapidly reaching  $100$  GeV for  $M_A = 700$  GeV. Note that the theoretical limits are not shown in this plot.

## B. $H$ decays

In this section we deal with the decays of the heavier CP-even Higgs boson. New contributions to the  $\rho$  parameter are avoided by setting  $M_A = M_{H^\pm} = 250$  GeV. Again, the constraint from  $B \rightarrow X_s \gamma$  is used. Then, we distinguish between two extreme situations. The first one, shown in Fig. 4, is for  $\sin(\beta - \alpha) = 0.1$ . In this case, the  $H$  couplings to the gauge bosons are close to the SM ones. Due to the small value of  $\sin(\beta - \alpha)$  the mass bound on the light Higgs can easily be evaded and we choose the mass  $M_h = 50$  GeV (though smaller masses are also allowed). Finally, this is the limit where the  $H$  couplings to  $W^\pm H^\mp$  and  $ZA$  are very small. In the plot shown in Fig. 4, on the left, we can distinguish

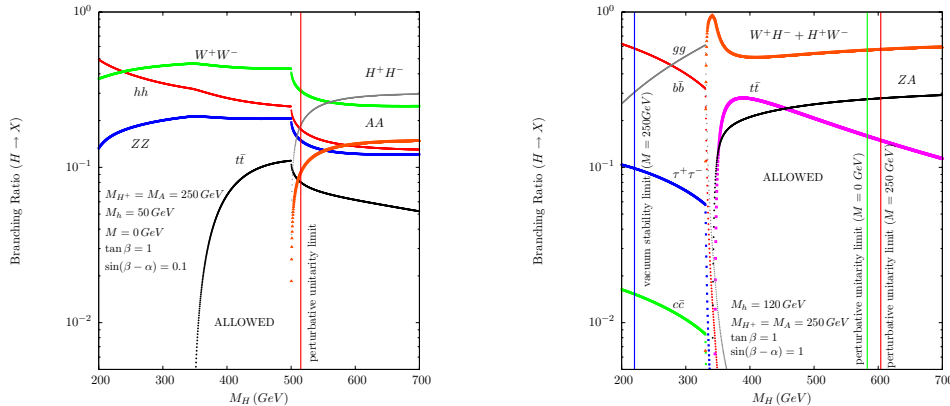


FIG. 4:  $H$  decays for  $M_A = M_{H^\pm} = 250$  GeV and  $\tan\beta = 1$ . On the left is the plot for  $M_h = 50$  GeV and  $\sin(\beta - \alpha) = 0.1$  while on the right we have  $M_h = 120$  GeV and  $\sin(\beta - \alpha) = 1$ . We show the perturbative unitarity and the vacuum stability limits, for  $M = 0$  GeV for the left plot and for  $M = 0$  GeV and  $M = 250$  GeV for the right plot.

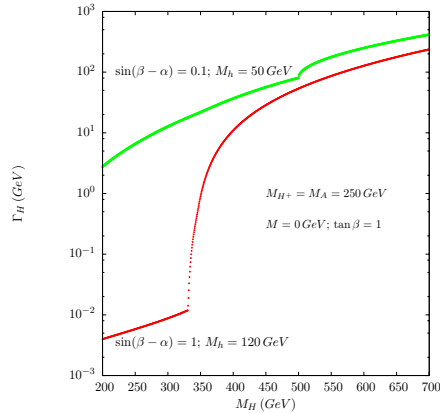


FIG. 5: Total width of the CP-even heavy Higgs state  $H$  for the parameter values presented in Fig. 4.

two interesting regions with new physics signatures. For small  $H$  masses,  $H \rightarrow hh, W^+W^-, ZZ$  can be the dominant decays. For large  $H$  masses, the decays to a pair of charged Higgs bosons and to a pair of CP-odd Higgs states dominate as soon as they are kinematically allowed. The larger  $\tan\beta$  is the more dominant these decays become. We also present the perturbative unitarity limit for  $M = 0 \text{ GeV}$ . As  $M$  grows the allowed region also grows but we may lose the decay to  $hh$ . For example, for  $M = 200 \text{ GeV}$  the decay to  $hh$  is negligible and in the low  $H$  mass region  $H \rightarrow W^+W^-$  always dominates. The other extreme situation is shown on the right hand side of Fig. 4 and occurs for  $\sin(\beta - \alpha) = 1$ . In this limit, the  $H$  couplings to the gauge bosons are exactly zero. Decays to the two light Higgs states are also suppressed but they could still play a role if the soft breaking parameter is different from zero. This is the limit where  $H$  couplings to  $W^\pm H^\mp$  and  $ZA$  are largest. Again we show perturbative unitarity and vacuum stability constraints for this case. Notice that the choice of  $\tan\beta = 1$  is heavily imposed by these bounds: for  $\tan\beta = 2$  and for the same set of parameters shown in the plot, the heavy CP-even Higgs mass is forced to be below  $\approx 350 \text{ GeV}$ . Even if  $M$  is raised to  $200 \text{ GeV}$  the bound only grows to  $\approx 400 \text{ GeV}$ . In Fig. 5 we show the total  $H$  width for the two situations presented in Fig. 4. When  $M_h = 50 \text{ GeV}$ , left plot in Fig. 4, the heavy Higgs is allowed to decay to other Higgs and gauge bosons and that is why the  $H$  width is SM-like for the same mass. In the other scenario the heavy CP-even Higgs is not allowed to decay to gauge bosons. It decays to two gluons and fermion pairs in the low mass region. Therefore the  $H$  width is much smaller. As soon as channels with Higgs and gauge boson open both widths converge to similar values.

### C. $H^\pm$ decays

This section is dedicated to charged Higgs boson decays. Again, we choose  $M_{H^\pm} = M_A$  to avoid the constraints from the  $\rho$  parameter. Once more we distinguish between two extreme cases regarding the value of  $\sin(\beta - \alpha)$ , which is the parameter that regulates the  $H^\pm$  coupling to other Higgses and gauge bosons. When  $\sin(\beta - \alpha)$  is such that the LEP bounds can be avoided there are mainly two competing decays for the allowed charged Higgs boson mass region:  $H^+ \rightarrow t\bar{b}$  and  $H^+ \rightarrow W^+h$ . In Fig. 6 we show the charged Higgs BRs for  $\sin(\beta - \alpha) = 0.1$  and  $M_h = 50 \text{ GeV}$  for two values of  $\tan\beta$ . It is clear that the decay  $H^+ \rightarrow W^+h$  is always important and becomes dominant for large values of  $\tan\beta$ . The other extreme case,  $\sin(\beta - \alpha) = 0.9$ , is plotted in Fig. 7. In this case the  $H^\pm$  coupling to the heavier CP-even Higgs boson becomes dominant relative to the light Higgs case and the decay  $H^+ \rightarrow W^+H$  is now the leading one for large values of  $\tan\beta$ . Again, we take  $M_H = 150 \text{ GeV}$ , though this value has no bearing on the final result except when we are in a region of large  $\tan\beta$  and large  $\sin(\beta - \alpha)$ . However, the large  $\tan\beta$  region is excluded by the perturbative unitarity constraints and therefore we will not consider this scenario. In Fig. 8 we show the total  $H^\pm$  width for the situations presented in Figs. 6 and 7. It is clear from the plot that the width does not depend so much on the parameters as happened for the previous cases. This is due to fact that all channel types are already allowed starting from  $M_{H^\pm} = 250 \text{ GeV}$ .

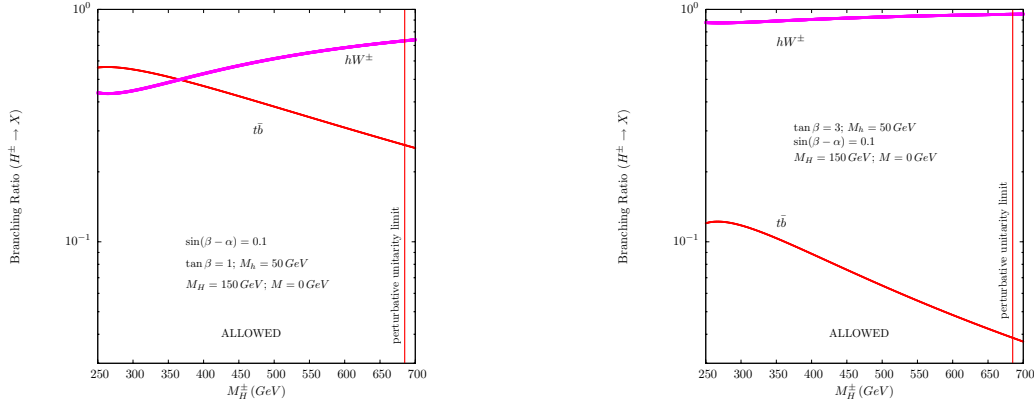


FIG. 6:  $H^\pm$  decays for  $M_h = 50 \text{ GeV}$ ,  $M_H = 150 \text{ GeV}$ ,  $M_A = M_{H^\pm}$  and  $\sin(\beta - \alpha) = 0.1$ . On the left is the plot for  $\tan \beta = 1$  while on the right we set  $\tan \beta = 3$ . Perturbative unitarity limits are shown.

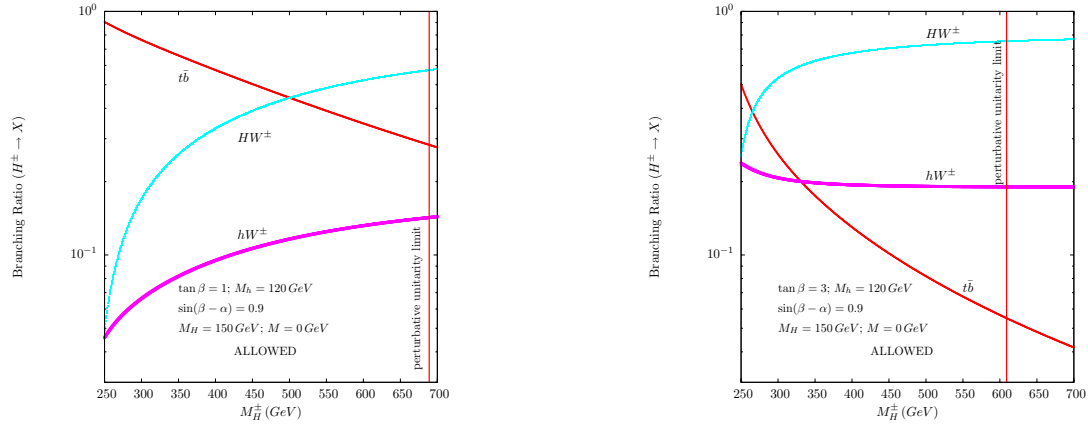


FIG. 7:  $H^\pm$  decays for  $M_h = 120 \text{ GeV}$ ,  $M_H = 150 \text{ GeV}$ ,  $M_A = M_{H^\pm}$  and  $\sin(\beta - \alpha) = 0.9$ . On the left is the plot for  $\tan \beta = 1$  while on the right we set  $\tan \beta = 3$ . Perturbative unitarity limits are shown.

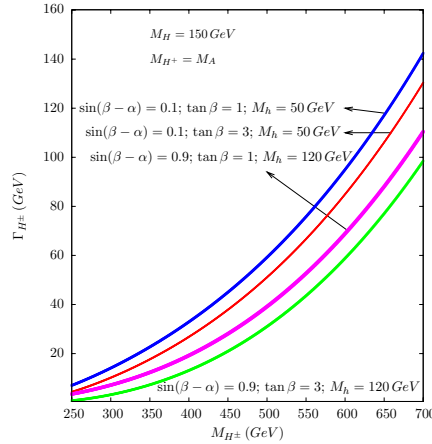


FIG. 8: Total width of the charged Higgs state  $H^\pm$  for the parameter values presented in Figs. 6 and 7.

## V. CONCLUSIONS

We have highlighted that in a Type II 2HDM there exist Higgs-to-Higgs decays which are prevented from occurring in its SUSY version, the MSSM, owing to the fact that the latter imposes stringent relations amongst the masses of the  $H$ ,  $A$  and  $H^\pm$  states, so that they are degenerate in mass over most of the

parameter space. As these modes typically involve decaying Higgs states that are rather heavy, they could be primary means available at the LHC (and much less so at the Tevatron) to dispell the MSSM hypothesis that assumes that the sparticle states are very heavy and beyond the kinematical reach of the collider. An analysis of Higgs pair production in the same spirit is now also in progress [31].

## APPENDIX A: YUKAWA COUPLINGS OF A TYPE II 2HDM

In this Appendix we present the Feynman rules for the Type II 2HDM Yukawa couplings. Hereafter, the label  $u$  refers to up-type quarks and neutrinos whilst  $d$  to down-type quarks and leptons. Also notice that the Goldstone bosons couple just like in the SM, so we do not report their fermionic interactions here. Finally, we define  $\gamma_L = (1 - \gamma_5)/2$  and  $\gamma_R = (1 + \gamma_5)/2$ . Using notation already introduced (apart from  $V_{ij}$  being the Cabibbo-Kobayashi-Maskawa matrix element in the quark sector and equating to 1 in the lepton case), one has:

$$\begin{aligned}
\bar{u}_i u_i h: & \quad -\frac{ig}{2M_W} \frac{\cos \alpha}{\sin \beta} m_{u_i} & \bar{d}_i d_i h: & \quad \frac{ig}{2M_W} \frac{\sin \alpha}{\cos \beta} m_{d_i} \\
\bar{u}_i u_i H: & \quad -\frac{ig}{2M_W} \frac{\sin \alpha}{\sin \beta} m_{u_i} & \bar{d}_i d_i H: & \quad -\frac{ig}{2M_W} \frac{\cos \alpha}{\cos \beta} m_{d_i} \\
\bar{u}_i u_i A: & \quad -\frac{g}{2M_W} \cot \beta m_{u_i} \gamma_5 & \bar{d}_i d_i A: & \quad -\frac{g}{2M_W} \tan \beta m_{d_i} \gamma_5 \\
\bar{u}_i d_j H^+: & \quad \frac{ig}{\sqrt{2}M_W} V_{ij} [\tan \beta m_{d_j} \gamma_R + \cot \beta m_{u_i} \gamma_L] & \bar{d}_i u_j H^-: & \quad \frac{ig}{\sqrt{2}M_W} V_{ij}^* [\tan \beta m_{d_i} \gamma_L + \cot \beta m_{u_j} \gamma_R]
\end{aligned}$$

**Acknowledgments** The authors thank Koji Tsumura and Mayumi Aoki for useful discussions. Also, they acknowledge financial support from the PMI2 Connect Initiative in the form of a Research Cooperation Grant. SM thanks SK, YM and KY for hospitality in Toyama while the latter thank the former for the same reason in Southampton. RS is supported by the FP7 via a Marie Curie Intra European Fellowship, contract number PIEF-GA-2008-221707.

- 
- [1] M. Drees, R. Godbole and P. Roy, “Theory and Phenomenology of Sparticles” (World Scientific Publishing Company, 2004).
- [2] H. E. Haber and G. L. Kane, Phys. Rept. **117** (1985) 75.
- [3] V. D. Barger, J. L. Hewett and R. J. N. Phillips, Phys. Rev. D **41** (1990) 3421.
- [4] J. F. Gunion, H. E. Haber, G. L. Kane and S. Dawson, “The Higgs Hunter’s Guide” (Westview Press, 2000) [Erratum arXiv:hep-ph/9302272].
- [5] A. Djouadi, Phys. Rept. **459** (2008) 1.
- [6] S. Moretti and W. J. Stirling, Phys. Lett. B **347** (1995) 291 [Erratum-ibid. B **366** (1996) 451].
- [7] A. Djouadi, J. Kalinowski and P. M. Zerwas, Z. Phys. C **70** (1996) 435.
- [8] Z. Kunszt, S. Moretti, and W. J. Stirling, Z. Phys. C **74** (1997) 479.
- [9] S. Moretti, J. Phys. G **28** (2002) 2567.
- [10] S. Kanemura, Y. Okada, E. Senaha and C. P. Yuan, Phys. Rev. D **70** (2004) 115002.
- [11] M. Aoki, S. Kanemura, K. Tsumura and K. Yagyu, in preparation; M. Aoki, S. Kanemura, O. Seto, arXiv:0807.0361 [hep-ph].
- [12] S. Schael *et al.* [ALEPH, DELPHI, L3 and OPAL Collaborations], Eur. Phys. J. C **47** (2006) 547.
- [13] V. M. Abazov *et al.* [D0 Collaboration], arXiv:0807.0859 [hep-ex]; CDF Collaboration, CDF Note 9322.
- [14] A. Denner, R. J. Guth, W. Hollik and J. H. Kuhn, Z. Phys. C **51** (1991) 695.
- [15] S. Eidelman *et al.* [Particle Data Group], Phys. Lett. B **592** (2004) 1.
- [16] A. Pomarol and R. Vega, Nucl. Phys. B **413** (1994) 3.
- [17] A. W. El Kaffas, O. M. Ogreid and P. Osland, arXiv:0709.4203 [hep-ph] and Phys. Rev. D **76** (2007) 095001.
- [18] M. Krawczyk and J. Zochowski, Phys. Rev. D **55** (1997) 6968; A. Dedes and H. E. Haber, JHEP **0105** (2001) 006.
- [19] See <http://lepewwg.web.cern.ch/LEPEWWG/>.
- [20] See <http://www-sld.slac.stanford.edu/sldwww/sld.html>.
- [21] D. S. Du, arXiv:0709.1315 [hep-ph].
- [22] J. Rosiek, Phys. Lett. B **252** (1990) 135; W. Hollik and T. Sack, Phys. Lett. B **284** (1992) 427; M. Krawczyk and D. Temes, Eur. Phys. J. C **44** (2005) 435.

- [23] P. H. Chankowski, M. Krawczyk and J. Zochowski, Eur. Phys. J. C **11** (1999) 661.
- [24] K. Cheung and O. C. W. Kong, Phys. Rev. D **68** (2003) 053003.
- [25] S. Kanemura, T. Kubota and E. Takasugi, Phys. Lett. B **313** (1993) 155.
- [26] A. G. Akeroyd, A. Arhrib and E. M. Naimi, Phys. Lett. B **490** (2000) 119; J. Horejsi and M. Kladiva, Eur. Phys. J. C **46** (2006) 81.
- [27] M. Sher, Phys. Rept. **179** (1989) 273; S. Kanemura, T. Kasai and Y. Okada, Phys. Lett. B **471** (1999) 182.
- [28] I. P. Ivanov, Phys. Rev. D **75** (2007) 035001 [Erratum-ibid. D **76** (2007) 039902].
- [29] P. M. Ferreira, R. Santos and A. Barroso, Phys. Lett. B **603** (2004) 219 [Erratum-ibid. B **629** (2005) 114].
- [30] V. D. Barger, J. L. Hewett and R. J. N. Phillips, Phys. Rev. D **41** (1990) 3421.
- [31] S. Kanemura, S. Moretti, Y. Mukai, R. Santos and K. Yagyu, in preparation.
- [32] To the extent that, for masses of the heavy Higgs states above 200  $GeV$  or so, a sort of decoupling occurs between these and the lightest Higgs boson of the MSSM, so that the latter resembles its SM counterpart.
- [33] While the  $H^\pm \rightarrow W^\pm h$  channel is kinematically possible in the MSSM, this only occurs with sizable rates in a  $\tan\beta$  region which is already excluded by experimental data.